List of Supplementary Material and Related Captions

Supplementary Material 1. $^{230}Th/^{234}U$ dating method.

Table DR1. Main known fissure ridge travertines in the world and related attributes.

Table DR2. Uranium content, uranium and thorium activity ratios, and age of travertines sampled in the Denizli basin for this work.

Table DR3. Oxygen and carbon stable isotope data of travertines sampled in the Denizli basin for this work.

Figure DR1. Ages (with error bars) of Denizli travertines (from this work and from Uysal et al., 2007, 2009) plotted over figure 1 from Wang et al. (2001). Travertines from Denizli basin are distinguished in banded (red diamonds for data from this work and green diamonds for data from Uysal et al., 2007, 2009) and bedded travertine (blue diamonds, only from this work). Vertical yellow bars indicate Younger Dryas (YD) and Heinrich paleoclimate events (H) (Wang et al., 2001). The band encompassed by the red dashed line indicates Last Glacial Maximum (LGM) (Mix et al., 2001). Also shown are $\delta^{18}O$ of Hulu Cave stalagmites (purple, green, and red), Greenland Ice (GISP2, 1997) (dark blue), and insolation (33°N June, July, and August) (Berger, 1978; Paillard et al., 1996) (black) versus time. Numbers indicate GISs and their correlation with Hulu data. The $\delta^{18}O$ values of the numbered peaks are reversed for Hulu (increasing down) in comparison with GISP2 (increasing up) (see Wang et al., 2001 for further details).

References

Berger, A., 1978, Long-term variations of daily insolation and quaternary climatic changes: Journal of the Atmospheric Science 35, 2362–2367.

GISP2, 1997, The Greenland Summit Ice Cores, National Snow and Ice Data Center, University of Colorado at Boulder, and the World Data Center-A for Paleoclimatology, National Geophysical Data Center, Boulder Colorado.

Mix, A.C., Bard, E., Schneider, R., 2001, Environmental processes of the ice age: land, oceans, glaciers (EPILOG). Quaternary Science Reviews 20 (4), p. 627–657.

Paillard, D., Labeyrie, L., and Yiou, P. (1996), Macintosh Program performs time-series analysis, Eos Transactions AGU, 77(39), 379, doi:10.1029/96EO00259.

Uysal, I.T., Feng, Y., Zhao, J.X., Altunel, E., Weatherley, D., Karabacak, V., Cengiz, O., Golding, S.D., Lawrence, M.G., and Collerson, K.D., 2007, U-series dating and geochemical tracing of late Quaternary travertine in co-seismic fissures: Earth and Planetary Science Letters, v. 257 (3–4), p. 450–462.

Uysal, I.T., Feng, Y., Zhao, J.X., Isik, V., Nuriel, P., and Golding, S.D., 2009, Hydrotermal CO2 degassing in seismically active zones during the Late Quaternary: Chemical Geology, v. 265, p. 442-454.

Wang, Y.J., Cheng, H., Edwards, R.L., An, Z.S., Wu, J.Y., Shen, C.C., and Dorale, J.A., 2001, A high-resolution absolute-dated late Pleistocene monsoon record from Hulu Cave, China: Science 294 (5550), 2345–2348.

Figure DR2. Ages (with error bars) of Denizli travertines (from this work and from Uysal et al., 2007, 2009) plotted over figure 1 from Fleitmann et al. (2009). Travertines from Denizli basin are distinguished in banded (red diamonds for data from this work and green diamonds for data from Uysal et al., 2007, 2009), and bedded travertine (blue diamonds, only from this work). (a-i) Vertical grey bars indicate Heinrich events (H) (Wang et al., 2001), YD is for Younger Dryas (Wang et al., 2001); the band encompassed by the red dashed line indicates Last Glacial Maximum (LGM) (Mix et al., 2001). See Fleitmann et al. (2009) for all the details about the $\delta^{18}O$ and $\delta^{13}C$ records, and U-Th dates worldwide.

References

Fleitmann, D., Cheng, H., Badertscher, S., Edwards, R.L., Mudelsee, M., Göktürk, O.M., Fankhauser, A., Pickering, R., Raible, C.C., Matter, A., Kramers, J., and Tüysüz, O., 2009, Timing and climatic impact of Greenland interstadials recorded in stalagmites from northern Turkey: Geophysical Research Letters, vol. 36, L19707, doi:10.1029/2009GL040050, 2009.

Mix, A.C., Bard, E., Schneider, R., 2001, Environmental processes of the ice age: land, oceans, glaciers (EPILOG). Quaternary Science Reviews 20 (4), p. 627–657.

Uysal, I.T., Feng, Y., Zhao, J.X., Altunel, E., Weatherley, D., Karabacak, V., Cengiz, O., Golding, S.D., Lawrence, M.G., and Collerson, K.D., 2007, U-series dating and geochemical tracing of late Quaternary travertine in co-seismic fissures: Earth and Planetary Science Letters, v. 257 (3–4), p. 450–462.

Uysal, I.T., Feng, Y., Zhao, J.X., Isik, V., Nuriel, P., and Golding, S.D., 2009, Hydrotermal CO2 degassing in seismically active zones during the Late Quaternary: Chemical Geology, v. 265, p. 442-454.

Wang, Y.J., Cheng, H., Edwards, R.L., An, Z.S., Wu, J.Y., Shen, C.C., and Dorale, J.A., 2001, A high-resolution absolute-dated late Pleistocene monsoon record from Hulu Cave, China: Science 294 (5550), 2345–2348.

Supplementary Material 1

^{230}Th/^{234}U dating method

The method is based on the extreme fractionation of the parent isotopes ^{238}U and ^{234}U from their long-lived daughter ^{230}Th in the hydrosphere. Uranium, markedly more soluble than Th in the surface and near-surface environments, is readily mobilized as the highly soluble uranyl ion (UO_2^{2+}) and its complexes, whereas Th is easily hydrolyzed and precipitated or adsorbed on detrital particles. Uranium is co-precipitated with $CaCO_3$ on exsolution of CO_2, while Th is generally negligible. In the absence of detrital Th, ^{230}Th only forms in situ by radioactive decay of co-precipitated U. In a closed system the extent to which the ^{230}Th/^{234}U activity ratio has returned towards unity is a function of time, taking into account also the state of disequilibrium between ^{234}U and ^{238}U (Kaufman and Broecker, 1965). About 500 mg of travertine samples were spiked with a mixed ^{236}U–^{229}Th tracer and dissolved in concentrated distilled HCl. The dried chloride was then converted to nitrate. U and Th were separated on miniaturized PTFE columns containing U-TEVA™ resin using HNO3 and HCl. As the Th eluate is strongly bound to rather volatile organic matter washed from the resin, the Th fraction was evaporated at <50°C to avoid loss by evaporation. Organic molecules from the resin were oxidized according to the protocol described in Tuccimei et al. (2010). After oxidation, U and Th samples were dissolved in 3 M HCl, and measured on a Nu Instruments™ multicollector plasma source mass spectrometer equipped with an APEX™ desolvating nebulizer. The WARP™ filter limiting access to one of the ion counters of the mass spectrometer is able to reduce the background on masses 230 and 229 to less than 0.5 ppm and less than 0.2 ppm of the peak height at mass 232, respectively. Measurement protocols are as described by Fleitmann et al. (2007). Activity ratios for MC-ICPMS data were calculated with the decay constants described in Cheng et al. (2000). The ages of all samples were calculated by means

of Isoplot/Ex (version 3.0), a plotting and regression program designed by Ludwig (2003) for radiogenic-isotope data.

Uranium content, uranium and thorium activity ratios, and the age of travertine are reported in Table DR2. Uranium abundances range from 6 to 392 ppb. Banded travertines from the Akkoy fissure ridge (the site with most dated samples) display uranium concentration higher than the values observed for bedded deposits. ($^{234}U/^{238}U$) activity ratios do not show large fluctuations and equal to 1.196 – 1.347, with the exception of sample Cuk1 (from Çukurbag fissure ridge) with a value of 1.435. The detrital content is negligible as evidenced by ($^{230}Th/^{232}Th$) activity ratios, always higher than 100, with the exception of sample Ko1 (from Kocabaş fissure ridge) where this ratio approaches 50. Therefore, no correction scheme is required to obtain a reliable age.

References

Cheng, H., Edwards, R.L., Hoff, J., Gallup, C.D., Richards, D.A., and Asmero, Y., 2000, The half-lives of uranium-234 and thorium-230: Chemical Geology 169, p. 17-33.

Fleitmann, D., Burns, S.J., Mangini, A., Mudelsee, M., Kramers, J., Villa, I.M., Neff, U., Al-Subbary, A.A., Buettner, A., Hippler, D., and Matter, A., 2007, Holocene ITCZ and Indian monsoon dynamics recorded in stalagmites from Oman and Yemen (Socotra): Quaternary Science Reviews 26, p. 170-188.

Kaufman, A., and Broecker, W.S., 1965, Comparison of 230Th and 14C ages of carbonate materials from Lakes Lahantan and Bonneville: Journal of Geophysical Research 70, p. 4039-4054.

Ludwig, K.R., 2003, Using Isoplot/Ex, Version 3. A GeochronologicalToolkit for Microsoft Excel: Berkeley Geochronology Ctr. Spec. Pub. 4.

Tuccimei, P., Soligo, M., Ginés, J., Ginés, A., Fornós, J., Kramers, J., and Villa, I.M., 2010, U-Th ages of phreatic overgrowths onspeleothems from coastal caves in Mallorca (Western Mediterranean): Earth Surface Processes and Landforms 35, p. 782-790.

Table DR1. Main known fissure ridge travertines in the world and related attributes.

(1) The term "isolated" refers to the occurrence of fissure ridges as single structures or in swarms.
(2) Note that the banded travertine occurs in the inner portion of fissure ridges and only in some cases it is visible.
(3) Not interpreted as fissure ridge but as "line of tufa cones" or "fossil spring deposits" deposited from hot thermal waters.

fissure ridge	locality	country	lat	long	tectonic setting	position to main fault	long-axis trend	length (m)	width (m)	height (m)	isolated (1)	observed banded travertine (2)	references
Kamara	Yenice (Denizli basin)	Turkey	N 38°03'24"	E 28°58'16"	extensional basin	hanging wall	N125°	63	15	6	no	yes	Cakir 1999
Çukurbağ	Pamukkale (Denizli basin)	Turkey	N 37°55'53"	E 29°06'58"	extensional basin	hanging wall	N85°	350	36	11	no	yes	Altunel & Hancock 1993a, Altunel & Karabacak 2005, Uysal et al. 2007, 2009
Çukurbağ 2	Pamukkale (Denizli basin)	Turkey	N 37°55'51"	E 29°07'04"	extensional basin	hanging wall	N77°	130	14	1	no	no	Altunel & Hancock 1993a
Akköy (Karakaya Hill)	Akköy (Denizli basin)	Turkey	N 37°56'56"	E 29°05'28"	extensional basin	hanging wall	N116° - N146°	1900	200	25	no	yes	Altunel & Hancock 1993a, Altunel & Karabacak 2005, Uysal et al. 2007, 2009
Karahayit	Karahayit (Denizli basin)	Turkey	N 37°57'26"	E 29°06'12"	extensional basin	hanging wall	N145°	600	200	7	no	yes	Altunel & Hancock 1993a, 1993b, 1996
Kizilseki Hill	Kizilseki Hill (Denizli basin)	Turkey	N 37°57'16"	E 29°05'55"	extensional basin	hanging wall	N147°	1200	220	35	no	yes	Altunel & Hancock 1993a, 1993b, 1996
Hanife Hill	Hanife Hill (Denizli basin)	Turkey	N 37°56'43"	E 29°06'14"	extensional basin	hanging wall	N113° - N161°	750	160	10	no	yes	Altunel & Hancock 1993a, 1993b, 1996
Kocabaş	Kocabaş (Denizli basin)	Turkey	N 37°48'39"	E 29°18'59"	extensional basin	hanging wall	N115° - N126°	2700	300	20	no	yes	Altunel & Karabacak 2005
Bal	Balkayasi (Gediz graben)	Turkey	N 38°22'07"	E 28°42'43"	extensional basin	hanging wall	N135°	350	25		no		Cakir 1999
Cambazli	Cambazli (Gediz graben)	Turkey	N 38°34'14"	E 27°50'21"	extensional basin	hanging wall		200	5	15	no	yes	Haluk Selim & Yanik 2009
Kirsehir	Kirsehir (Central Anatolia)	Turkey	N 39°07'50"	E 34°07'52"	extensional basin	hanging wall	N170°	800	30	4	no	yes	Atabey 2002, Temiz et al. 2009, Uysal et al. 2009
Ihlara	Ihlara Valley (Central Anatolia)	Turkey	N 38°17'15"	E 34°14'23"	volcanic field						no	yes	Karabacak & Altunel 2005
Sicak Çermik	Sivas area (Central Turkey)	Turkey	N 39°44'55"	E 36°42'58"	pull apart		N30°	1600			no	yes	Piper et al. 2007, Mesci et al. 2008
Delikkaya	Sivas area (Central Turkey)	Turkey	N 39°44'55"	E 36°42'58"	pull apart		N150°	500			no	yes	Piper et al. 2007, Mesci et al. 2008
Sarikaya	Sivas area (Central Turkey)	Turkey	N 39°44'55"	E 36°42'58"	pull apart		N115°	750			no	yes	Piper et al. 2007, Mesci et al. 2008
Terme S. Giovanni	Rapolano Terme (Siena)	Italy	N 43°16'46"	E 11°35'31"	extensional basin	hanging wall	N117°	250	30	10	yes	no	Guo & Riding 1999, Brogi 2004, Brogi & Capezzuoli 2009
Abano Terme	Abano Terme (Padova)	Italy	N 45°21'09"	E 11°46'38"	volcanic field	hanging wall	N120°				yes	no	Zampieri et al. 2010
Nymphopetres (3)	Lakes Volvi and Langada (Mygdonia basin)	Greece	N 40°41'52"	E 23°19'30"	extensional basin	hanging wall	NNW-SSE		3	5	no		Pavlides & Kilias 1987, Traganos et al. 1995, Hancock et al. 1999
Hot Tub Ridge	Bridgeport (California)	U.S.A.	N 38°14'45"	W 119°12'18"	extensional basin	hanging wall	N204° - N221°	165	7	4.5	no	yes	Chesterman & Kleinhampl 1991, Hancock et al. 1999
White Elephant Back Terrace	Mammoth Hot Springs (Wyoming)	U.S.A.	N 44°57'49"	W 110°42'47"	volcanic field	hanging wall	N45°	235	15	8	no	yes	Bargar 1978
Pyramid Lake (3)	Pyramid Lake (Nevada)	U.S.A.	N 40°08'47"	W 119°40'44"	extensional basin		N145°	2000	165	10-65	no		Benson 1994, Hancock et al. 1999
Searles Lake (3)	Searles Lake (California)	U.S.A.	N 35°43'27"	W 117°20'37"	extensional basin	hanging wall	N-S				no		Scholl & Taft 1964, Hancock et al. 1999
Soda Dam	Jemez Springs (New Mexico)	U.S.A.	N 35°47'29"	W 106°41'11"	volcanic field	hanging wall	N240°	100	25	15	no		Chafetz & Folk 1984, Goff & Shevenell 1987
Crystal Geyser system	Paradox Basin (Utah)	U.S.A.	N 38°56'18"	W 110°08'08"	extensional basin	footwall	WNW-ESE	80	70	3	no	yes	Shipton et al. 2004, 2005, Dockrill & Shipton 2010
San Antonio Texcala	San Antonio Texcala (Puebla)	Mexico	N 18°24'01"	W 97°26'43"								yes	Michalzik et al. 2001
Zerka Mai'in	Madaba (Dead Sea region)	Jordan	N 31°36'11"	E 35°36'21"									Khoury et al. 1984
Hammam Meskoutine	Hammam Meskoutine	Algeria	N 36°27'42"	E 07°16'10"							no		Pentecost & Viles 1994, Pentecost 2005

References

Altunel, E., and Hancock P.L., 1996, Structural attributes of travertine-filled extensional fissures in the Pamukkale plateau, western Turkey: International Geology Review, v. 38, p. 768-777.

Altunel, E., and Hancock, P.L., 1993a, Active fissuring and faulting in Quaternary travertines at Pamukkale, western Turkey, *in* Stewart, I.S., Vita-Finzi, C., and Owen, L.A., Neotectonics and Active Faulting: Zeitschrift fuer Geomorphologie Supplement, v. 94, p. 285-302.

Altunel, E., and Hancock, P.L., 1993b, Morphology and structural setting of Quaternary travertines at Pamukkale, Turkey: Geological Journal, v. 28, p. 335–346.

Altunel, E., and Karabacak, V., 2005, Determination of horizontal extension from fissure-ridge travertines: a case study from the Denizli Basin, southwestern Turkey: Geodinamica Acta, v. 18, p. 333–342.

Atabey, E., 2002, The formation of fissure ridge type laminated travertine-tufa deposits microscopical characteristics and diagenesis, Kirsehir Central Anatolia: Mineral Research Exploration Bulletin (MTA), v. 123-124, p. 59–65.

Bargar, K.E., 1978, Geology and thermal history of Mammoth Hot Springs, Yellowstone National Park, Wyoming: U. S. Geological Survey Bulletin, v. 1444, p. 1–55.

Benson, L., 1994, Carbonate deposition, Pyramid Lake Subbasin, Nevada: 1. Sequence of formation and elevation distribution of carbonate deposits (Tufas): Palaeogeography, Palaeoclimatology, Palaeoecology, v. 109, p. 55-87.

Brogi, A., 2004, Faults linkage, damage rocks and hydrothermal fluid circulation: tectonic interpretation of the Rapolano Terme travertines (southern Tuscany, Italy) in the context of the Northern Apennines Neogene-Quaternary extension: Eclogae Geologicae Helvetiae, v. 97, p. 307–320, doi:10.1007/s00015-004-1134-5.

Brogi, A., and Capezzuoli, E., 2009, Travertine deposition and faulting: the fault-related travertine fissure-ridge at Terme S. Giovanni, Rapolano Terme (Italy): International Journal of Earth Sciences Geol Rundsch, v. 98, p. 931– 947, doi:10.1007/s00531-007-0290-z.

Çakır, Z., 1999, Along-strike discontinuity of active normal faults and its influence on Quaternary travertine deposition; examples from western Turkey: Turkish Journal of Earth Sciences, v. 8, p. 67–80.

Chafetz, H.S., and Folk, R.L., 1984, Travertines: depositional morphology and the bacterially constructed constituents: Journal Sedimentary Petrology, v. 54, p. 289–316.

Chesterman, C.W., and Kleinhampl, F.J., 1991, Travertine Hot Springs, Mono County, California: California Geology, California Department of Conservation, Division of Mines and Geology, August 1991, v. 44, no. 8, p. 171-182.

Dockrill, B., and Shipton, Z.K., 2010, Structural controls on leakage from a natural CO2 geologic storage site: central Utah, U.S.A.: Journal of Structural Geology, v. 32, issue 11, p. 1768-1782, doi: 10.1016/j.jsg.2010.01.007.

Goff, F., and Shevenell, L., 1987, Travertine deposits of Soda Dam, New Mexico, and their implications for the age and evolution of the Valles caldera hydrothermal system: Geological Society of America Bulletin, v. 99, 292-302, August 1987.

Guo, L., and Riding, R., 1999, Rapid facies changes in Holocene fissure ridge hot spring travertines, Rapolano Terme, Italy: Sedimentology, v. 46, p. 1145–1158.

Haluk Selim, H., and Yanik, G., 2009, Development of the Cambazlı (Turgutlu/MANISA) fissure-ridge-type travertine and relationship with active tectonics, Gediz Graben, Turkey: Quaternary International, v. 199, issues 1-2, p. 157-163, doi:10.1016/j.quaint.2008.04.009.

Hancock, P.L., Chalmers, R.M.L., Altunel, E., and Çakir, Z., 1999, Travitonics: using travertine in active fault studies: Journal of Structural Geology, v. 21, p. 903–916.

Karabacak, V., and Altunel, E., 2005, Relationship between travertine deposition and volcanic activity: *in* Özkul, M., Yağiz, S., and Jones, B., eds., Proceedings of 1st International Symposium on Travertine, September 21-25, 2005, Pamukkale University (Denizli, Turkey).

Khoury, H., Salameh, E. and Udluft, P., 1984, On the Zerka Ma'in (Therma Kallirhoes) travertine/Dead Sea (hydrohemistry, geochemistry and isotopic composition): Neues Jahrbuch für Geologie und Paläontologie, Monatshefte, v. 8, p. 472–484.

Mesci, L.B., Gürsoy, H., and Tatar, 2008, The evolution of travertine masses in the Sivas Area (Central Turkey) and their relationships to active tectonics: Turkish Journal of Earth Sciences, v. 17, p. 219–240.

Michalzik, D., Fischer, R., Hernandez, D., and Oezen, D., 2001, Age and origin of the "Mexican Onyx" at San Antonio Texcala (Puebla, Mexico): Geologische Beiträge Hannover, v. 2, p. 79-89.

Pavlides, S.B., and Kilias, A.A., 1987, Neotectonic and active faults along the Serbomacedonian zone (SE Chalkidiki, northern Greece): Annales Tectonicae, v. 1, p. 97-104.

Pentecost, A., 2005, Travertine: Springer-Verlag, Berlin Heidelberg, 445 pp.

Pentecost, A., and Viles, H.A., 1994, A review and reassessment of travertine classification: Géographie physique Quaternaire, v. 48, p. 305–314.

Piper, J.D.A., Mesci, L.B., Gürsoy, H., Tatar, O., and Davies, CJ., 2007, Palaeomagnetic and rock magnetic properties of travertine: Its potential as a recorder of geomagnetic palaeosecular variation, environmental change and earthquake activity in the Sıcak Çermik geothermal field, Turkey: Physics of the Earth and Planetary Interiors, v. 161, p. 50–73, doi:10.1016/j.pepi.2007.01.006.

Scholl, D.W., and Taft, W.H., 1964, Algae, contributors to the formation of calcareous tufa, Mono Lake, California: Journal Sedimentary Petrology, v. 34, p. 309–319.

Shipton, Z.K., Evans, J.P., Kirchner, D., Kolesar, P.T., Williams, A.P. and Heath, J., 2004, Analysis of CO2 leakage through "low-permeability" faults from natural reservoirs in the Colorado Plateau, southern Utah: *in* Baines, S.J. and Worden, R.H., eds., Geological storage of carbon dioxide: Geological Society, London, Special Publications, no. 233, p. 43-58.

Shipton, Z.K., Evans, J.P., Dockrill, B., Heath, J., Williams, A., Kirchner, D., and Kolesar, P.T., 2005, Natural leaking CO2-charged systems as analogs for failed geologic sequestration reservoirs: *in* Thomas, D., and Benson, S.M., eds., Carbon Dioxide Capture for Storage in Deep Geologic Formations; Results from the CO2 Capture Project, v. 2, Elsevier Science, p. 699-712.

Temiz, U., Gökten, E., and Eikenberg, J., 2009, U/Th dating of fissure ridge travertines from the Kirsehir region (Central Anatolia Turkey): structural relations and implications for the Neotectonic development of the Anatolian block: Geodinamica Acta, v. 22/4, p. 201-213.

Traganos, G., Jux, U., and Steuber, T., 1995, Isotopic characteristics of geothermal waters and fossil spring deposits in Mygdonia Basin, Northern Greece: Geothermics, v. 24, no. 1, p. 61-80.

Uysal, I.T., Feng, Y., Zhao, J.X., Altunel, E., Weatherley, D., Karabacak, V., Cengiz, O., Golding, S.D., Lawrence, M.G., and Collerson, K.D., 2007, U-series dating and geochemical tracing of late Quaternary travertine in co-seismic fissures: Earth and Planetary Science Letters, v. 257 (3–4), p. 450–462.

Uysal, I.T., Feng, Y., Zhao, J.X., Isik, V., Nuriel, P., and Golding, S.D., 2009, Hydrotermal CO2 degassing in seismically active zones during the Late Quaternary: Chemical Geology, v. 265, p. 442-454.

Table DR2. Uranium content, uranium and thorium activity ratios and the age of travertine. Errors are always quoted as 2σ .

fissure ridge	sample	travertine type	lat	long	ppb U	($^{230}Th/^{232}Th$)	($^{234}U/^{238}U$)	($^{230}Th/^{234}U$)	age (ka)
Kamara	Ka2	banded	N 38°03’24”	E 28°58’16”	392.49 ± 0.67	150.62 ± 2.13	1.287 ± 0.002	0.015 ± 0.001	1.7 ± 0.1
Kamara	Ka4	banded	N 38°03’24”	E 28°58’16”	383.94 ± 0.68	136.52 ± 2.01	1.347 ± 0.002	0.023 ± 0.001	2.5 ± 0.1
Çukurbağ	Cuk1	banded	N 37°55’54”	E 29°06’58”	93.24 ± 0.19	225.02 ± 4.32	1.435 ± 0.004	0.199 ± 0.002	24.1 ± 0.3
Çukurbağ	Pa5	bedded	N 37°55’53”	E 29°06’56”	27.08 ± 0.07	250 ± 2.87	1.285 ± 0.005	0.432 ± 0.007	60 ± 1
Akköy	Ak15	banded	N 37°57’02”	E 29°05’22”	96.94 ± 0.17	187 ± 2.24	1.196 ± 0.002	0.237 ± 0.011	29.3 ± 1.6
Akköy	Ak16	banded	N 37°57’02”	E 29°05’22”	195.53 ± 0.33	173.65 ± 2.41	1.243 ± 0.002	0.180 ± 0.004	20.2 ± 0.5
Akköy	Ak17	banded	N 37°57’02”	E 29°05’22”	290.17 ± 0.49	284 ± 5.24	1.241 ± 0.001	0.138 ± 0.002	16.3 ± 0.3
Akköy	Ak21	banded	N 37°56’57”	E 29°05’26”	117.91 ± 0.20	201 ± 3.54	1.232 ± 0.002	0.225 ± 0.023	27.5 ± 3.2
Akköy	Ak22	banded	N 37°56’57”	E 29°05’26”	271 ± 0.46	333.39 ± 6.41	1.236 ± 0.002	0.179 ± 0.001	21.4 ± 0.1
Akköy	Ak23	banded	N 37°56’54”	E 29°05’26”	355.71 ± 0.60	102.23 ± 2.02	1.214 ± 0.002	0.195 ± 0.004	23.5 ± 0.6
Akköy	Ak24	bedded	N 37°56’54”	E 29°05’26”	70.13 ± 0.13	198 ± 2.04	1.220 ± 0.003	0.392 ± 0.009	53.4 ± 1.6
Akköy	Ak26	banded	N 37°56’56”	E 29°05’27”	259.93 ± 0.44	125.68 ±1.82	1.226 ± 0.001	0.200 ± 0.003	24.1 ± 0.4
Akköy	Ak27	bedded	N 37°56’56”	E 29°05’27”	31.75 ± 0.15	127.70 ± 1.96	1.237 ± 0.005	0.286 ± 0.023	36.4 ± 3
Kocabaş	Ko1	banded	N 37°48’39”	E 29°19’01”	12.94 ± 0.03	50.26 ± 0.99	1.203 ± 0.004	1.100 ± 0.020	≥ 350
Kocabaş	Ko2	banded	N 37°48’39”	E 29°18’56”	21.82 ± 0.05	321 ± 4.56	1.122 ± 0.003	0.786 ± 0.012	160 ± 5
Kocabaş	Ko4	banded	N 37°48’39”	E 29°19’00”	6.55 ± 0.02	297 ± 3.87	1.218 ± 0.006	1.007 ± 0.035	≥ 350

Table DR3. Oxygen and carbon stable isotope data.

fissure ridge or fault	sample	travertine type	lat	long	$\delta^{18}O$ (PDB) ‰	$\delta^{13}C$ (PDB) ‰	references
Kamara	Ka2	banded	N 38°03’24”	E 28°58’16”	-13.60	2.92	this work
Kamara	Ka4	banded	N 38°03’24”	E 28°58’16”	-13.10	3.34	this work
Kamara	Ka5	bedded	N 38°03’24”	E 28°58’16”	-8.34	5.01	this work
Kamara	Ka6	bedded	N 38°03’24”	E 28°58’16”	-12.30	4.38	this work
Kamara	Ka7	banded	N 38°03’24”	E 28°58’16”	-13.20	3.19	this work
Çukurbağ	Cuk1	banded	N 37°55’54”	E 29°06’58”	-14.10	5.79	this work
Çukurbağ	Cuk5	bedded	N 37°55’53”	E 29°06’56”	-9.74	6.43	this work
Çukurbağ	Pa5	bedded	N 37°55’53”	E 29°06’56”	-9.82	7.83	this work
Akköy	Ak2	banded	N 37°56’54”	E 29°05’26”	-7.14	6.17	this work
Akköy	Ak3	bedded	N 37°56’52”	E 29°05’30”	-10.30	5.35	this work
Akköy	Ak3	banded	N 37°56’52”	E 29°05’30”	-11.00	5.27	this work
Akköy	Ak17	banded	N 37°57’02”	E 29°05’22”	-12.20	4.55	this work
Akköy	Ak18	bedded	N 37°57’02”	E 29°05’22”	-11.30	4.70	this work
Akköy	Ak19	banded	N 37°57’02”	E 29°05’22”	-11.85	4.97	this work
Akköy	Ak21	banded	N 37°56’57”	E 29°05’26”	-8.75	6.46	this work
Akköy	Ak22	banded	N 37°56’57”	E 29°05’26”	-9.23	7.11	this work
Akköy	Ak23	banded	N 37°56’54”	E 29°05’26”	-9.12	7.51	this work
Akköy	Ak24	bedded	N 37°56’54”	E 29°05’26”	-9.86	5.80	this work
Akköy	Ak25	bedded	N 37°56’54”	E 29°05’26”	-9.59	5.34	this work
Akköy	Ak25	banded	N 37°56’54”	E 29°05’26”	-10.40	4.71	this work
Akköy	Ak26	banded	N 37°56’55”	E 29°05’27”	-8.78	7.52	this work
Akköy	Ak27	bedded	N 37°56’55”	E 29°05’27”	-9.56	6.21	this work
Kocabaş	Ko1	banded	N 37°48’39”	E 29°19’01”	-14.00	5.42	this work
Kocabaş	Ko2	bedded	N 37°48’39”	E 29°18’56”	-9.67	5.04	this work
Kocabaş	Ko2	banded	N 37°48’39”	E 29°18’56”	-11.10	5.51	this work
Pamukkale	PI-1	banded	N 37°55’44”	E 29°06’56”	-16.3	5.8	Uysal et al., 2007
Akköy	PII-1	banded	N 37°56’52”	E 29°05’35”	-15.2	4.7	Uysal et al., 2007
Akköy	PII-3	banded	N 37°56’52”	E 29°05’35”	-14.4	4.8	Uysal et al., 2007
Hanife Hill	PIII-1	banded	N 37°56’47”	E 29°06’19”	-14.5	4.9	Uysal et al., 2007
Hanife Hill	PIII-2	banded	N 37°56’47”	E 29°06’19”	-12.4	4.7	Uysal et al., 2007
Pamukkale	PIV-1	banded	N 37°55’47”	E 29°06’35”	-14.3	5.7	Uysal et al., 2007
Pamukkale	PIV-2	banded	N 37°55’47”	E 29°06’35”	-15.0	5.6	Uysal et al., 2007
Pamukkale Range-front Fault	HB1	banded	N 37°57’12”	E 29°06’57”	-14.6	4.7	Uysal et al., 2007
Pamukkale Range-front Fault	HCE	banded	N 37°57’08”	E 29°06’59”	-11.3	5.1	Uysal et al., 2007

References

Uysal, I.T., Feng, Y., Zhao, J.X., Altunel, E., Weatherley, D., Karabacak, V., Cengiz, O., Golding, S.D., Lawrence, M.G., and Collerson, K.D., 2007, U-series dating and geochemical tracing of late Quaternary travertine in co-seismic fissures: Earth and Planetary Science Letters, v. 257 (3–4), p. 450–462.

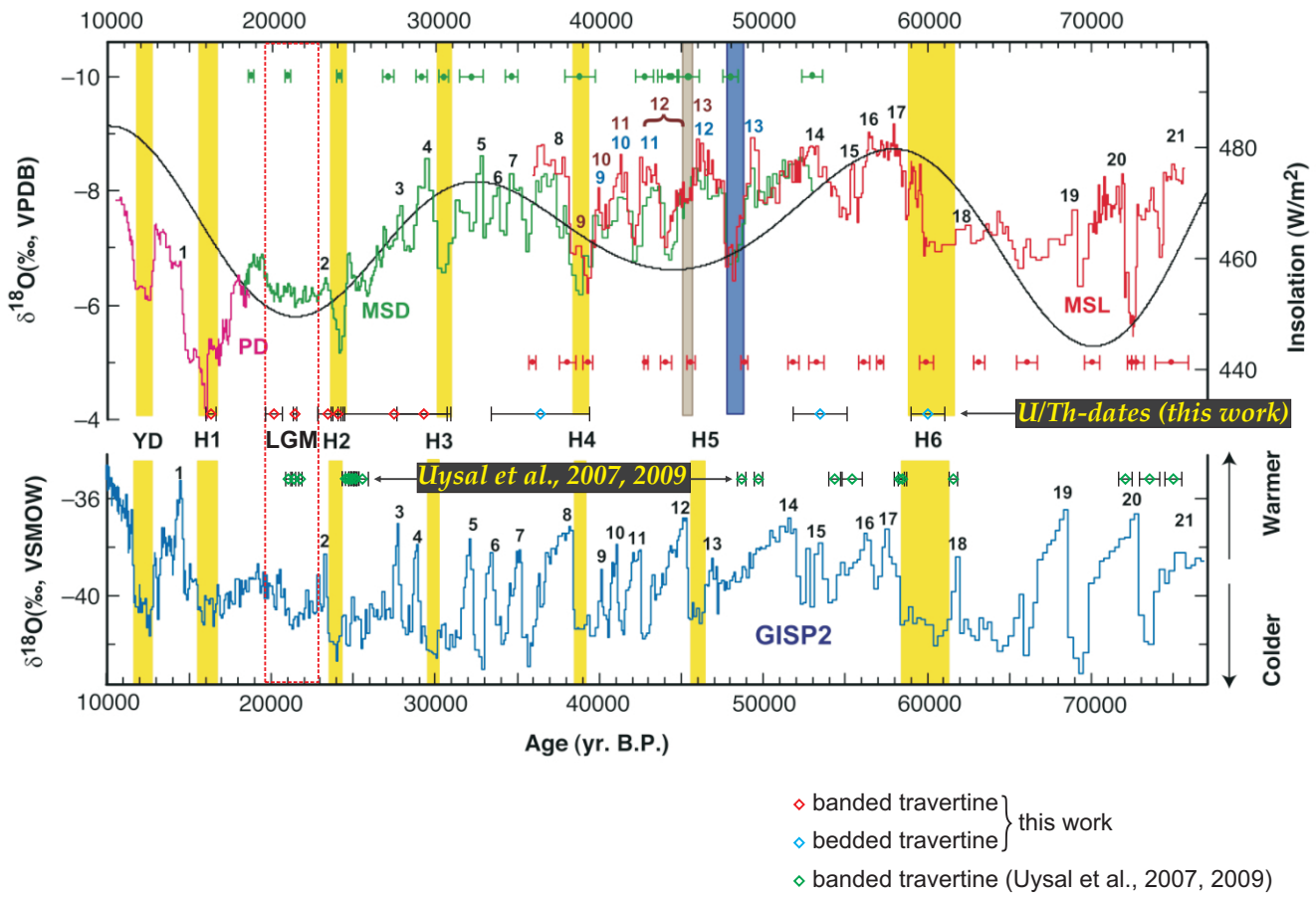

banded travertine } this work
bedded travertine
banded travertine (Uysal et al., 2007, 2009)

Figure DR1

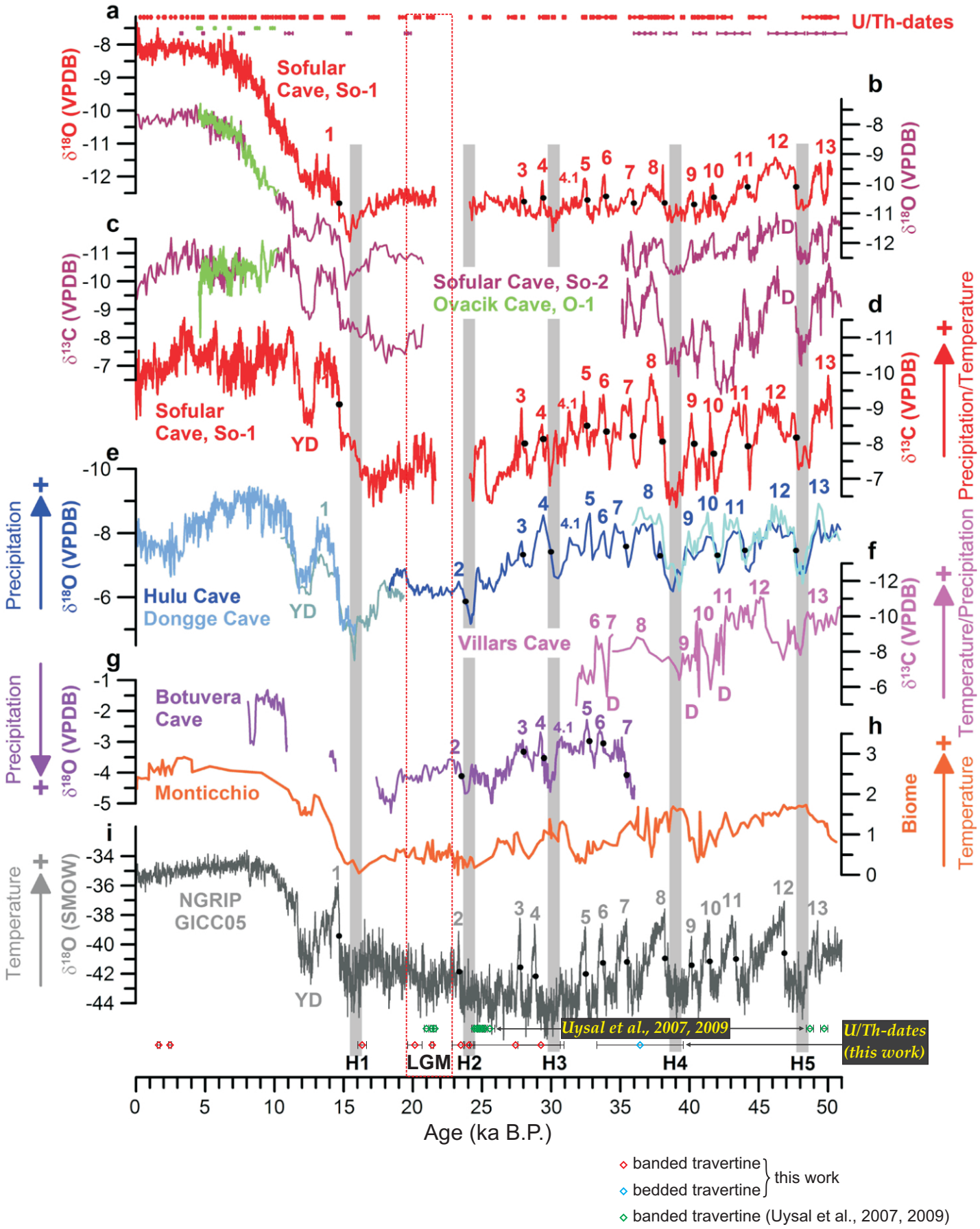
a
U/Th-dates
Sofular Cave, So-1
δ18O (VPDB)
b
δ18O (VPDB)
c
δ13C (VPDB)
Sofular Cave, So-2
Ovacik Cave, O-1
Sofular Cave, So-1
YD
d
δ13C (VPDB)
Precipitation/Temperature
e
δ18O (VPDB)
Precipitation
Hulu Cave
Dongge Cave
YD
f
δ13C (VPDB)
Temperature/Precipitation
Villars Cave
g
δ18O (VPDB)
Precipitation
Botuvera Cave
Monticchio
h
Biome
Temperature
i
δ18O (SMOW)
Temperature
NGRIP GICC05
YD
Uysal et al., 2007, 2009
U/Th-dates (this work)
H1
LGM
H2
H3
H4
H5
Age (ka B.P.)
banded travertine
bedded travertine
this work
banded travertine (Uysal et al., 2007, 2009)

Figure DR2